HIGH-INTENSITY DEMONSTRATIONS IN THE J-PARC 3-GeV RCS

H. Hotchi*, M. Kinsho, K. Hasegawa, N. Hayashi, Y. Hikichi, S. Hiroki, J. Kamiya, K. Kanazawa, M. Kawase, M. Nomura, N. Ogiwara, R. Saeki, P.K. Saha, A. Schnase, Y. Shobuda, T. Shimada, K. Suganuma, H. Suzuki, H. Takahashi, T. Takayanagi, O. Takeda, F. Tamura, N. Tani, T. Togashi, T. Ueno, M. Watanabe, Y. Watanabe, K. Yamamoto, M. Yamamoto, Y. Yamazaki, H. Yoshikawa, and M. Yoshimoto,
Japan Atomic Energy Agency (JAEA), Tokai, Naka, Ibaraki, 319-1195 Japan
A. Ando, H. Harada, Y. Irie, C. Ohmori, K. Satou, Y. Yamazaki, and M. Yoshii,
High Energy Accelerator Research Organization (KEK), Tsukuba, Ibaraki, 305-0801 Japan

Abstract

The J-PARC RCS was commissioned in October 2007. Via the initial beam tuning and underlying beam studies with low intensity beams, we demonstrated high-intensity beam operations (100-300 kW equivalent intensities) including the beam painting injection scheme. In this paper, we describe beam study results for the high intensity beams together with the corresponding space-charge simulations, and also some issues that we found in the demonstrations.

INTRODUCTION

The J-PARC accelerator complex [1] comprises a 400-MeV linac, a 3-GeV rapid cycling synchrotron (RCS), a 50-GeV main ring synchrotron (MR) and several experimental facilities (a materials and life science experimental facility; MLF, a hadron experimental hall, and a neutrino beam line to Kamioka). The J-PARC beam commissioning started in November 2006 and it has well proceeded as planned from the linac toward the downstream facilities. The RCS was commissioned in October 2007. Six run cycles through February 2008 were dedicated to RCS commissioning, for which we completed the initial beam tuning and underlying beam studies with low intensity beams [2]. Then since May 2008 the extracted RCS beam has been delivered to the MR and MLF for their beam commissioning. Since then, while the priority has been given to MR and MLF beam tuning, the RCS also continues further beam tuning and studies toward higher beam intensity. Now the RCS is in transition from the first commissioning phase to the next challenging stage, and our efforts hereafter will be focused on higher power operations.

The RCS has two functions as a proton driver for the MLF and as an injector to the MR. A negative hydrogen ion (H^-) beam from the linac is delivered to the RCS injection point, where it is multi-turn charge-exchange injected with a carbon stripper foil. The RCS accelerates the injected beam up to 3 GeV at 25 Hz repetition. The RCS design parameters are listed in Table 1. With the current injection energy of 181 MeV, the RCS aims at providing at least 0.3 MW output beam power. After upgrading the linac energy to 400 MeV by adding an annular coupled structure (ACS) linac in the future, the RCS will aim at 1 MW output. One of key issues to achieve such a high intensity operation is to decrease and localize beam losses. In high intensity proton machines like the RCS, the space-charge effect would pose a severe limitation on the achievable beam intensity. In order to mitigate the space-charge effect, the RCS adopts a multi-turn painting injection scheme in both the transverse and longitudinal phase spaces. The permissible range of intensity loss for 0.3 MW output operation with 181 MeV injection energy, which is determined by the current collimator capacity of 4 kW, is 22% at the injection energy. On the other hand, the allowable intensity loss for 1 MW output operation with 400 MeV injection energy is 3% if assuming the same collimator limit at the injection energy. The above two operations give an equivalent space-charge effect at each injection energy. Therefore, to achieve 0.3 MW output with less than 3% intensity loss for 181 MeV injection energy is the first matter leading to the realization

Table 1: RCS Design Parameters.

Circumference	348.333 m
Superperiodicity	3
Injection energy	181 MeV*
Extraction energy	3 GeV
Repetition rate	25 Hz
Ramping pattern	Sinusoidal
Injection period	0.5 ms (235 turns)
Harmonic number	2
Number of bunches	2
Output beam power	0.3-0.6 MW*
Number of particles per pulse	2.5-5.0$\times10^{13}$
Transition energy	9.21 GeV
Momentum acceptance	$\pm1\%$
Ring acceptance	486 π mm mrad
Collimator acceptance	324 π mm mrad
Transverse painting emittance	216 π mm mrad
Longitudinal beam emittance	2.5 eVs
Bunching factor at injection	0.4
Space-charge tune shift at injection for 0.3 MW output	-0.14

*The injection energy will be upgraded to 400 MeV by adding an ACS linac section in the future, for which the design output beam power is 1 MW.

* hotchi.hideaki@jaea.go.jp

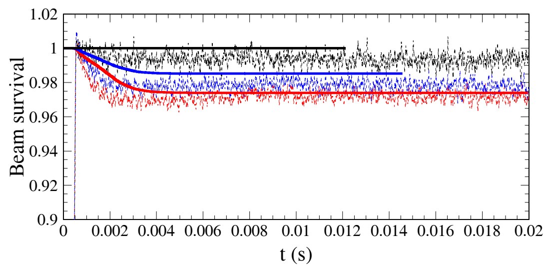

Figure 1: Beam survival measured with DCCT for 100 kW (black), 225 kW (blue) and 300 kW (red) equivalent intensity beams with no beam painting. Solid curves are the results from the corresponding space-charge simulations.

of 1 MW output with 400 MeV injection energy.

INTENSITY DEPENDENCE OF THE BEAM LOSS

Via a series of basic beam tuning measurements and underlying beam studies mainly related to single-particle behavior of low intensity beams, we demonstrated high-intensity beam operations with 5-15 mA peak and 0.5 ms long linac pulse. Figure 1 shows beam intensity losses measured with a DC current transformer (DCCT) for 100 kW (5 mA peak/0.5 ms long/53% chopper beam-on duty factor), 225 kW (15 mA/0.5 ms/40%) and 300 kW (15 mA/0.5 ms/53%) equivalent intensity beams. This demonstration was carried out with no beam painting (center injection), for which the observed intensity losses were 0.5-3% depending on the beam intensity only appearing around the injection energy. In addition, the particle loss during the beam accumulation process has to be taken into account, which mainly come from the beam scattering on the charge-exchange foil. In the center injection, the circulating beam hits the foil every turn during injection. In addition, the current fall time of the injection-orbit bump (0.5 ms) is longer than the design (0.18 ms) and also the size and positioning of the foil is still not optimized. These circumstances increase the frequency of the foil hitting. The current number of the foil hits is 125, which is 6 times larger than the design, and its resultant beam loss during the charge accumulation process was experimentally confirmed to be around 1% [3]. Solid curves in the figure show results from the corresponding space-charge simulations using a fully 3D particle-in-cell code called SIMPSONS [4] including the following realistic conditions; (1) transverse Twiss functions and emittances of the injection beam, (2) multipole field components for all the ring magnets, (3) field and alignment errors, (4) static leakage fields from the extraction beam line, (5) edge focusing effect of the injection-orbit bump magnets, and (6) chromatic correction at the injection with DC power supplies, where (1)-(4) are based on measurements. While the calculated ones give a similar intensity dependence as the measured ones, there still exists some discrepancy especially around the injection energy region. In these simulations, the foil scattering effect during injection is not yet included. The foil scattering ought to cause beam halo, through which it should contribute to particle losses especially at the early stage of acceleration after the beam accumulation is complete. Therefore the agreement of the measured and calculated intensity losses may get much better if the foil scattering effect is included in our simulation.

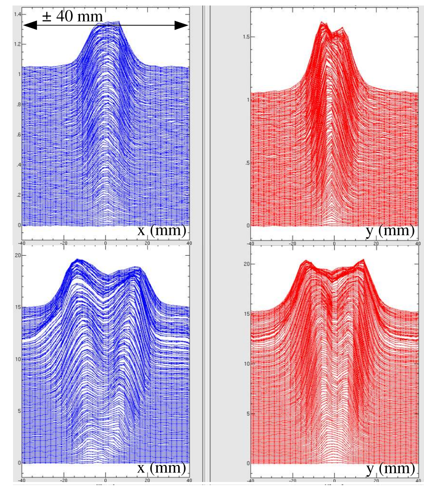

Figure 2: Horizontal (left) and vertical (right) beam profile mountain views measured over the injection period (0.5 ms) with IPM, where the upper ones show those for the center injection, and the lower ones are with the transverse beam painting (correlated painting). The painting emittance was set at 150π mm mrad for both the horizontal and vertical planes.

BEAM LOSS REDUCTION BY THE BEAM PAINTING

We performed the transverse and longitudinal painting injection scheme aiming at beam loss reduction at the early stage of acceleration observed above.

In the horizontal plane, the injection beam was painted from the middle to the outside of the RCS beam ellipse along its major axis in phase space (x,x') by sweeping the closed orbit, while in the vertical plane, the injection beam was moved from the middle to the outside (correlated painting) or from the outside to the middle (anti-correlated painting) along the y' axis. Figure 2 shows beam profile mountain views measured with residual gas ionization profile monitors (IPM) for the center and correlated painting injections, where the painting emittance was set at 150π mm mrad for both the horizontal and vertical planes.

On the other hand, the longitudinal beam painting [5] was performed by combination of the momentum-offset injection scheme, in which the rf frequency had an offset, and superposing a second harmonic rf voltage to widen and flatten the rf bucket. The phase sweep of the second harmonic rf voltage relative to the fundamental one was also employed so that the shape of the rf bucket was dynamically changed during the injection process. Figure 3 shows longitudinal beam profile mountain views measured using a wall current monitor (WCM) without and with the longi-

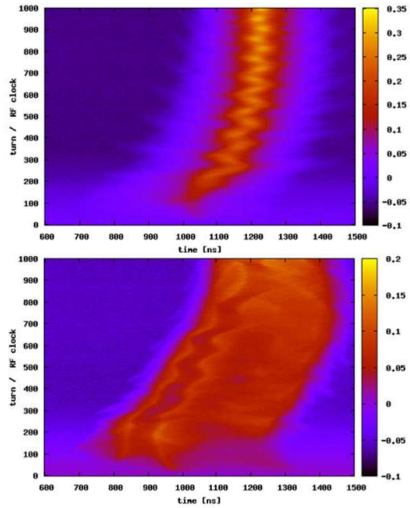

Figure 3: Longitudinal beam profile mountain views measured for the injection period (0.5 ms) using WCM without (upper) and with (lower) the longitudinal beam painting.

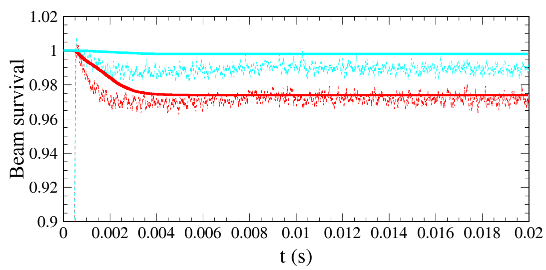

Figure 4: Beam survival measured with DCCT for 300 kW equivalent intensity beam without (red) and with (right blue) the beam painting injection. Solid curves are the results from the corresponding space-charge simulations.

tudinal painting. In this case of longitudinal painting, the second harmonic component has an amplitude of 80% of the fundamental voltage, and its phase is sweeping from -80 to 0 degrees. The rf frequency offset corresponds to a -0.1% momentum offset.

Figure 4 shows beam intensity losses measured for 300 kW equivalent intensity beam without and with the painting scheme mentioned above. As clearly shown in the figure, the beam intensity loss was well improved by controlling the charge density of the beam.

ISSUES AND FUTURE PROSPECT

While the DCCT displayed the beam intensity loss only around the injection energy, the beam loss monitors more sensitively detected particle losses at the missing-bend cells with dispersion maximum. Figure 5(a) show beam loss monitor signals at the missing-bend cell measured for 100 kW-equivalent intensity beam with no beam painting. As shown in the figure, the particle loss was detected mainly at the middle and late stage of the acceleration process, and it was very sensitive for the tune variation (Fig. 5(b)) during acceleration. These situations implies that some of beam particles with large amplitudes in the longitudinal phase space are lost at the dispersion peak point due to some aberration in the transverse phase space. For such a particle loss, the full chromatic correction over the acceleration process, which improve the dynamic aperture for the off-momentum particle, will be effective. However, in the RCS, the chromaticity is now corrected at the injection energy with DC-excited sextupoles. Therefore the effect of the chromatic correction gradually fade out during acceleration. Such a beam loss at higher energy region will cause critical machine activations, even if its amount is small. While the particle loss was minimized by optimizing the tune variation as for 100-kW equivalent intensity beam with the center injection, the situation will get severe when introducing the beam painting for higher intensity beams, because the beam painting logically increases the number of particles with large amplitudes for both the transverse and longitudinal spaces. For this concern, we plan to introduce AC power supplies for the chromatic correction sextupoles in the near future.

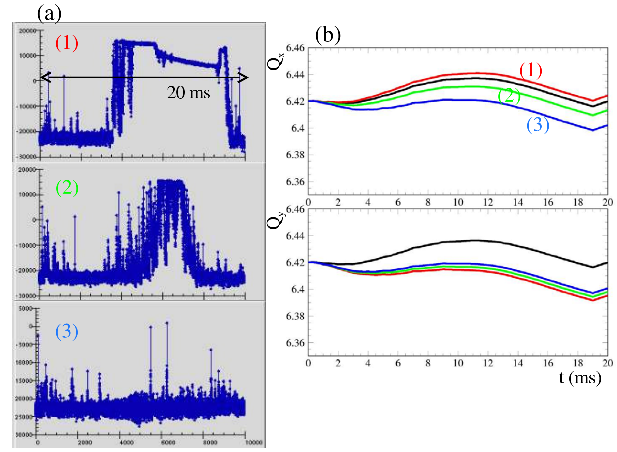

Figure 5: Beam loss monitor signals (a) at the missing-bend cell detected for 100 kW equivalent intensity beam with no beam painting for several tune variations during acceleration (b).

The emphasis of the RCS beam tuning hereafter will be focused on "stable" high-power beam operations, for which further beam loss reduction and localization through the global optimization for various correlated parameters including the beam painting scheme are essential.

REFERENCES

[1] "Accelerator Technical Design Report for High-Intensity Proton Accelerator Facility Project", JAERI-Tech 2003-044.

[2] H. Hotchi *et al.*, "Beam commissioning of the 3-GeV rapid cycling synchrotron of the Japan Proton Accelerator Research Complex", to be published in Phys. Rev. ST Accel. Beams (2009).

[3] P.K. Saha *et al.*, in Proceedings of PAC2009.

[4] S. Machida and M. Ikegami, "Simulation of Space Charge Effects in a Synchrotron", AIP Conf. Proc. 448, p.73, 1998.

[5] F. Tamura *et al.*, Phys. Rev. ST Accel. Beams **12**, 041001 (2009).